Original Article | Neurointervention

http://dx.doi.org/10.3348/kjr.2015.16.6.1353
pISSN 1229-6929 · eISSN 2005-8330
Korean J Radiol 2015;16(6):1353-1363

Korean Journal of Radiology
KJR

Subtraction MR Venography Acquired from Time-Resolved Contrast-Enhanced MR Angiography: Comparison with Phase-Contrast MR Venography and Single-Phase Contrast-Enhanced MR Venography

Jinhee Jang, MD[1], Bum-Soo Kim, MD[1], Jinkyeong Sung, MD[2], Bom-Yi Kim, MD[1], Hyun Seok Choi, MD[1], So-Lyung Jung, MD[1], Kook-Jin Ahn, MD[1]

[1]Department of Radiology, Seoul St. Mary's Hospital, College of Medicine, The Catholic University of Korea, Seoul 06591, Korea; [2]Department of Radiology, St. Vincent's Hospital, College of Medicine, The Catholic University of Korea, Suwon 16247, Korea

Objective: To evaluate the image characteristics of subtraction magnetic resonance venography (SMRV) from time-resolved contrast-enhanced MR angiography (TRMRA) compared with phase-contrast MR venography (PCMRV) and single-phase contrast-enhanced MR venography (CEMRV).

Materials and Methods: Twenty-one patients who underwent brain MR venography (MRV) using standard protocols (PCMRV, CEMRV, and TRMRA) were included. SMRV was made by subtracting the arterial phase data from the venous phase data in TRMRA. Co-registration and subtraction of the two volume data was done using commercially available software. Image quality and the degree of arterial contamination of the three MRVs were compared. In the three MRVs, 19 pre-defined venous structures (14 dural sinuses and 5 cerebral veins) were evaluated. The signal-to-noise ratio (SNR) and contrast-to-noise ratio (CNR) of the three MRVs were also compared.

Results: Single-phase contrast-enhanced MR venography showed better image quality (median score 4 in both reviewers) than did the other two MRVs ($p < 0.001$), whereas SMRV (median score 3 in both reviewers) and PCMRV (median score 3 in both reviewers) had similar image quality ($p \geq 0.951$). SMRV (median score 0 in both reviewers) suppressed arterial signal better than did the other MRVs (median score 1 in CEMRV, median score 2 in PCMRV, both reviewers) ($p < 0.001$). The dural sinus score of SMRV (median and interquartile range [IQR] 48, 43–50 for reviewer 1, 47, 43–49 for reviewer 2) was significantly higher than for PCMRV (median and IQR 31, 25–34 for reviewer 1, 30, 23–32 for reviewer 2) ($p < 0.01$) and did not differ from that of CEMRV (median and IQR 50, 47–52 for reviewer 1, 49, 45–51 for reviewer 2) ($p = 0.146$ in reviewer 1 and 0.123 in reviewer 2). The SNR and CNR of SMRV (median and IQR 104.5, 83.1–121.2 and 104.1, 74.9–120.5, respectively) were between those of CEMRV (median and IQR 150.3, 111–182.6 and 148.4, 108–178.2) and PCMRV (median and IQR 59.4, 49.2–74.9 and 53.6, 43.8–69.2).

Conclusion: Subtraction magnetic resonance venography is a promising MRV method, with acceptable image quality and good arterial suppression.

Index terms: *Time-resolved MR venography; Subtraction; Phase-contrast MR venography; Contrast-enhanced MR venography*

Received March 5, 2015; accepted after revision July 21, 2015.
Bum-Soo Kim received research funding from Bayer Healthcare, Guerbet, Dongkook Pharmaceuticals which were not relevant to this study.
Corresponding author: Bum-Soo Kim, MD, Department of Radiology, Seoul St. Mary's Hospital, College of Medicine, The Catholic University of Korea, 222 Banpo-daero, Seocho-gu, Seoul 06591, Korea.
• Tel: (822) 2258-6239 • Fax: (822) 599-6771 • E-mail: bkim.neurorad@gmail.com

INTRODUCTION

There are a number of MR methods for visualizing the venous systems of the head and neck area. These include single-phase contrast-enhanced MR venography (CEMRV), time-of-flight MR venography (TOF MRV), and phase-contrast MR venography (PCMRV) (1-3). Recent reports suggested the feasibility of time-resolved contrast-enhanced MR angiography (TRMRA) for evaluating venous structures in the head and neck (4-9). TRMRA images acquired during the first pass of the contrast bolus are similar to those obtained using digital subtraction angiography. Those studies used latter-phase image sets of TRMRA to assess the venous system (5-7).

Because there is a trade-off between temporal and spatial resolution in TRMRA, currently available TRMRA techniques are based primarily on view-sharing methods (10, 11). Although those methods enabled the increased frame rate of multiphasic images, they elongated the temporal footprint compared with the image update time on acquired multiphasic images (12). Temporal footprint is the duration over which any views used for a single image are acquired with view-sharing methods (12). Usage of multiple shared samplings over time elongated the temporal footprint. A considerably long temporal footprint resulted in poor arterial-venous separation, and consequently, the venous phase of current TRMRA was not a vein-only image but an image with simultaneous the visualization of arteries and veins. In this study, we presented a practical method for removing the arterial contamination on TRMRA venous phase images by subtraction. The purpose of this study was to evaluate the image characteristics of the subtraction MR venography (SMRV) compared with standard MR venography (MRV) images.

MATERIALS AND METHODS

Patients

This retrospective study was approved by our Institutional Review Board and complied with Health Insurance Portability and Accountability Act guidelines. The requirement to obtain informed consent was waived. From May 2013 to November 2013, 25 consecutive patients underwent MRV imaging at our hospital. One patient was excluded because of a severe motion artifact of TRMRA, and three were excluded because of loss of source data. A total of 21 patients (9 men and 12 women; mean age, 47.6 ± 13.7 years; range, 21–73 years) were included. Clinical indications for MRVs were variable and included preoperative evaluation of intracranial venous system (n = 15), suspected dural sinus thrombosis (n = 3), follow-up after diagnosis of dural sinus thrombosis (n = 2), and clinically suspected intracranial hypertension (n = 1).

Standard MR Venography Acquisition

All scans were performed using a 3T system (MAGNETOM Verio, Siemens AG, Healthcare Sector, Erlangen, Germany) with a 16-channel head and neck coil. The standard MRV protocol in our hospital includes PCMRV, CEMRV, and TRMRA. TRMRA was performed after PCMRV and CEMRV for hemodynamic information; we used vendor-standard protocols for PCMRV and CEMRV. Before positioning the patient, a 20-gauge cannula was inserted into an antecubital vein and connected to an MR-compatible electronic power injector (Spectris; Medrad Inc., Pittsburgh, PA, USA). Three-dimensional PCMRV images were acquired sagittally for the velocity encoding (VENC) values of 20 cm/s. Flow was encoded along all three orthogonal directions. A total of 144 slices with a 0.9 mm thickness and no interslice gap were centered as a single volume at the internal occipital protuberance in order to cover the torcular region, the transverse and sigmoid sinuses, the jugular bulbs and the initial portion of the jugular veins. Image parameters included repetition time/echo time/flip angle = 43.3 msec/6.85 msec/15°, 256 x 256 for the frequency/phase encoding matrix, with a numer of excitation (NEX) of 1, no flow compensation, and a 300 Hz/pixel bandwidth. An isotrophic 0.9 x 0.9 x 0.9 mm^3 voxel was acquired on 230 x 230 x 130 mm^3 field of view. The generalized autocalibrating partially parallel acquisitions (GRAPPA) parameters were set to an acceleration factor of 3 in the phase encoding direction with 24 reference k-space lines for calibration. The total scan time was 4 minutes 20 seconds.

For CEMRV, non-contrast and contrast-enhanced datasets were obtained using the same parameters except for contrast infusion. After intravenous injection of 0.1 mmol/kg of gadobutrol (Gadovist, Bayer Healthcare, Berlin, Germany) at 1.5 mL/s, followed by a 20 mL saline flush at the same rate, acquisition of the enhanced dataset was started manually as soon as the contrast agent was visible in the superior sagittal sinus on sagittal two-dimensional real-time fluoroscopy. Pre- and post-contrast acquisition was performed in the sagittal plane using a

Korean Journal of Radiology
KJR

fast gradient recalled echo sequence with elliptic centric k-space reordering (13). A total of 256 slices with a 0.6 mm thickness and no interslice gap were centered as a similar volume of PCMRV. Image parameters included repetition time/echo time/flip angle = 4.32 msec/1.64 msec/23°, 384 x 384 for the frequency/phase encoding matrix, a NEX of 1, and 470 Hz/pixel bandwidth. A 0.6 x 0.6 x 0.6 mm^3 isotrophic voxel was acquired on 230 x 230 x 150 mm^3 field of view. The GRAPPA parameters were set to an acceleration factor of 3 in the phase encoding direction with 24 reference k-space lines for calibration. The total acquisition time was 2 minute 27 seconds. CEMRV data was acquired by subtracting the pre-contrast and contrast-enhanced images.

TRMRA Acquisition and Post-Processing for Subtraction MR Venography

Time-resolved contrast-enhanced MR angiography was performed using the time-resolved angiography with stochastic trajectories (TWIST) technique after intravenous injection of a low dose (0.03 mmol/kg bolus at a flow rate of 1.5 mL/sec followed by a 20 cc saline flush at the same rate) of gadobutrol (14). TRMRA images were acquired in the coronal plane. Image parameters included repetition time/echo time/flip angle = 2.82 msec/0.99 msec/16°, 256 x 256 for the frequency/phase encoding matrix, a NEX of 1, and 540 Hz/pixel bandwidth. The acquired voxel size was 1.6 x 1.6 x 1.5 mm^3 on 400 x 400 x 190 mm^3 field of view. The GRAPPA parameters were set to an acceleration factor of 6 (3 in the phase-encoding direction and 2 in the slice-encoding direction) with 24 reference k-space lines for calibration. For the TWIST sequence, values of 8% for A (size of the central k-space region) and 20% for B (sampling density in the peripheral region) were used (10, 11, 14). A total of 60 seconds was covered with a temporal resolution of 0.98 seconds after interpolation. The temporal footprint was eight seconds.

Subtraction MR venography was obtained by post-processing the TRMRA data. After reviewing the time-series of the coronal and sagittal maximal intensity projection (MIP) TRMRA images, a neuroradiologist chose two phases from each patient's TRMRA (Fig. 1A, B), a phase just before the visualization of the right internal jugular vein (phase A; Fig. 1A, thin line on Fig. 1D) and another phase with peak opacification of the right internal jugular vein (phase B; Fig. 1B, thick line on Fig. 1D). The A and B phases were selected for each patient based on the evaluation of his or her TRMRA images with 30 mm^3 region of interest (ROI) on the mid-portion of the right internal jugular vein (black circle on Fig. 1B). After automated co-registration of the volume data for those two phases, a voxel-by-voxel subtraction was performed (phase B–phase A). Negative values were considered zero. Acquired volume data were used for variable image reconstructions, such as rotational MIP images (Fig. 1C) and thin slice multi-planar reformation (MPR) images. Image data were processed using commercially available software (Aquarius iNtuition,

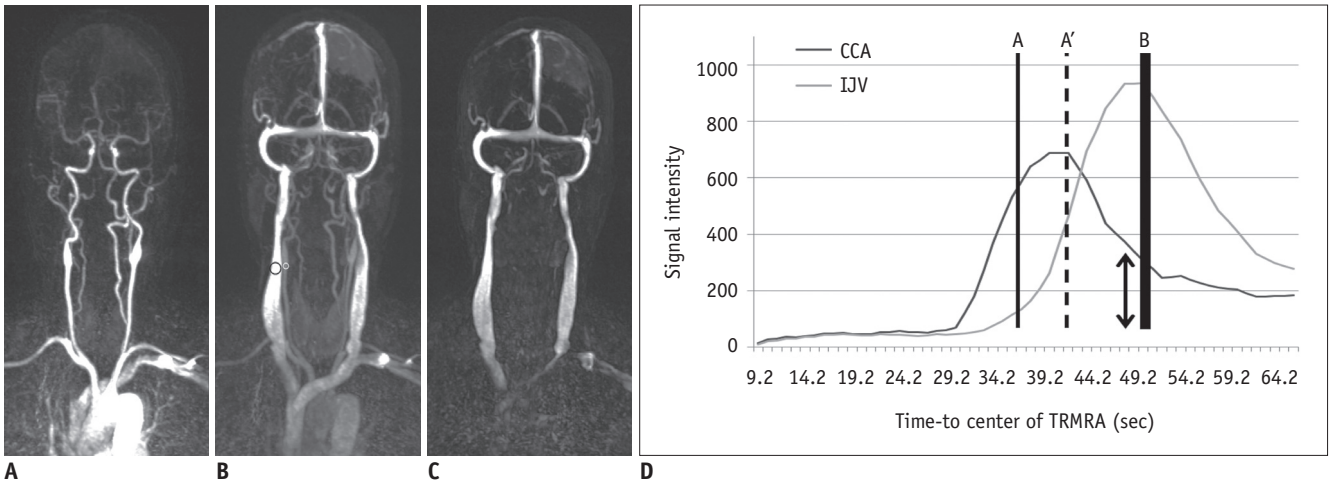

Fig. 1. Representative case for choosing optimal phase for SMRV from TRMRA of 64-year-old female.
On time-intensity curve **(D)** of right common carotid artery (CCA; black curve, white circle in **B**) and internal jugular vein (IJV; gray curve, black circle in **B**), signal characteristics of phases **A** and **B** were identified. Phase A **(A)** corresponds to time point of start of venous opacification (thin line), not arterial peak phase (dashed line). Phase B (thick line) had maximum venous structure signal. Phase B **(B)** shows substantial arterial signal, which is not desirable in MRV images. Acquired SMRV **(C)** image shows that arterial signal was clearly removed and cavernous and inferior petrosal sinuses were clearly visualized. SMRV = subtraction MR venography, TRMRA = time-resolved contrast-enhanced MR angiography

TeraRecon, Inc., Foster City, CA, USA).

Image Assessment

After randomizing the order of total 63 sets of three different MRVs, two experienced neuroradiologists who were blinded to patient clinical information assessed the horizontal and vertical rotational MIP images of MRVs. Axial thin-slice MPR images were assessed to confirm suspicious or inconclusive findings on rotational MIP images. The reviewers first evaluated the general image quality on a four-point Likert scale (0, non-diagnostic; 1, suboptimal and limited diagnostic value; 2, acceptable quality; 3, good image quality). The presence of arterial contamination was assessed on a four-point scale (0, no arterial contamination; 1, arterial visualization, less intense than venous structures; 2, arterial visualization, similar intensity with venous structure; 3, arterial visualization, higher intensity than venous structures). The reviewers also scored 19 pre-defined venous structures (superior sagittal sinus, inferior sagittal sinus, right and left internal cerebral veins, right and left basal veins of Rosenthal, vein of Galen, straight sinus, torcular herophili, right and left cavernous sinuses, right and left inferior petrosal sinuses, right and left transverse sinuses, right and left sigmoid sinuses, and right and left jugular bulbs) on a five-point scale that had been introduced in previous studies; 4 for intense and continuous visualization, 3 for faint and continuous visualization, 2 for non-continuous visualization with small gap, 1 for non-continuous visualization with large gap, and 0 for non-visualization (6, 7). Cerebral vein score was calculated by summing the scores of five cerebral veins (right and left internal cerebral veins, right and left basal veins of Rosenthal, and vein of Galen). Dural sinus score was calculated by summing the scores of 14 dural sinuses. In addition, total vein score was calculated by summing all 19 venous segments. To assess the intra-observer reliability of qualitative assessment, the same assessment was done by the first reviewer after three months in random order to avoid recall bias.

To assess quantitative image quality, ROIs were drawn on the mid-sagittal images of the three different MRVs by a neuroradiologist. A ROI was placed for the signal measurement of the proximal portion of the superior sagittal sinus. Then, another ROI of the same size was placed at the anterior aspect of first ROI but not including vascular structures. The mean signals of the superior sagittal sinus (SI_{SSS}) and background tissue (SI_{tissue}) were obtained from each ROI. To determine background noise, three ROIs of the same size were placed in air, anterior to the frontal bone, posterior to the occipital bone, and posterior to the neck. The mean of the standard deviations of these three measurements were used for estimate of background noise (7), because background noise is not uniform in parallel imaging (15, 16). The signal-to-noise ratio (SNR) and contrast-to-noise ratio (CNR) were calculated using the following equations: $SNR = SI_{SSS} / Noise$, $CNR = (SI_{SSS} - SI_{tissue}) / Noise$. Measurements were taken using ImageJ (ver 1.47, U.S. National Institutes of Health, Bethesda, MD, USA, http://imagej.nih.gov/ij/).

Statistical Analysis

Inter- and intra-observer reliability for assessing image quality and arterial contamination scores were evaluated by linear weighted κ statistics. Inter- and intra-observer reliability of dural sinus score, cerebral vein score and overall score were assessed by intraclass correlation coefficient. Scores for image quality and arterial contamination for the three MRV methods were compared using the non-parametric Friedman test. In addition, dural sinus score, cerebral vein score, and total vein score of the three MRVs were compared using Friedman test. Quantitative results including the SNR and CNR of the three MRV methods were also compared with the Friedman test. Post hoc analysis was conducted using the Wilcoxon signed rank test with Bonferroni correction. Statistical analysis was performed using commercially available software (MedCalc, Mariakerke, Belgium).

RESULTS

Subtraction magnetic resonance venography images were generated successfully for all 21 patients. In general, the total post-processing time was shorter than ten minutes including review of the MIP images of TRMRA, optimal phase selection, and subtraction. There were individual variations in the times of phases A (mean, 28.5 ± 7.6 seconds; median, 31.9; interquartile range (IQR), 23.9–35.9) and B (mean, 41.4 ± 7.5 seconds; median, 42.7; IQR, 36.2–47.9) among the 21 patients. However, the mean difference between phases A and B was more consistent among patients (mean, 12.9 ± 3.6 seconds; median, 12; IQR, 10–15) than the time-to-center of phases A or B.

The inter-observer reliability of the image quality scores was good in all three MRVs (κ = 0.611, 0.638, and

Korean Journal of Radiology
KJR

0.644, for PCMRV, CEMRV, and SMRV, respectively), and the intra-observer reliability of the image quality scores were also good in all three MRVs (κ = 0.774, 0.788, and 0.644, for PCMRV, CEMRV, and SMRV, respectively). Inter- and intra-observer variability of arterial contamination scores was good to excellent (κ = 0.679, 0.647, and 1 for inter-observer reliability of PCMRV, CEMRV, and SMRV, respectively, and κ = 0.838, 0.824, and 1 for intra-observer reliability of PCMRV, CEMRV, and SMRV respectively). Intra-observer variability of dural sinus score, cerebral vein score and total vein score was excellent (intraclass correlation coefficients were between 0.950 and 0.967). Inter-observer variability of dural sinus score, cerebral vein score and total vein score was good to excellent (intraclass correlation coefficient were between 0.817 and 0.949).

The image quality of the three MRV methods was statistically different in both reviewers (p < 0.001). Post hoc analysis suggested that CEMRV (median score 4 in both reviewers) had better image quality than the other MRV techniques (Table 1). Image quality of SMRV (median score 3 in both reviewers) was comparable with that of PCMRV (median score 3 in both reviewers) (p = 0.999). In terms of arterial signal suppression, SMRV (median score 0 in both reviewers) showed significantly better suppression than other two MRV methods (p < 0.001). There was no CEMRV or PCMRV without arterial signal contamination. Specifically, PCMRV showed similar or stronger arterial structure signals than venous structures in 20 patients. In contrast, SMRV showed only one case of arterial contamination, and it was weaker than the venous signal.

There were significant differences in total vein scores, dural sinus scores and cerebral vein scores in the three MRVs (Table 2). Post hoc tests revealed the highest total vein scores for CEMRV (median and IQR 68, 63–70 and 66, 61–70 in reviewer 1 and 2, respectively), which were significantly different from the other MRVs in both reviewers. In addition, SMRV (median and IQR 62, 60–67 in reviewer 1, 63, 57–64 in reviewer 2) had significantly higher total vein scores than PCMRV (39, 34–45 and 37, 32–42 in each reviewer, respectively). This tendency was same

Table 1. Image Quality and Arterial Contamination on Venography

	PCMRV	CEMRV	SMRV	*P*
Reviewer 1				
Arterial contamination (score)*				< 0.001
No arterial contamination (0)	0	0	20	
Arterial signal < venous signal (1)	1	15	1	
Arterial signal ≈ venous signal (2)	10	5	0	
Arterial signal > venous signal (3)	10	1	0	
Image quality (score)†				< 0.001
Good image quality (3)	0	19	0	
Acceptable quality (2)	18	1	20	
Suboptimal, limited diagnostic value (1)	3	1	1	
Non-diagnostic (0)	0	0	0	
Reviewer 2				
Arterial contamination (score)*				< 0.001
No arterial contamination (0)	0	0	20	
Arterial signal < venous signal (1)	1	13	1	
Arterial signal ≈ venous signal (2)	8	7	0	
Arterial signal > venous signal (3)	12	1	0	
Image quality (score)†				< 0.001
Good image quality (3)	0	19	0	
Acceptable quality (2)	18	1	19	
Suboptimal, limited diagnostic value (1)	3	1	2	
Non-diagnostic (0)	0	0	0	

P values were acquired using Friedman test. *Post-hoc analysis suggested that SMRV was better than other MRV techniques (p < 0.001), †Post-hoc analysis suggested that CEMRV was better than other MRV techniques (p < 0.001). Score of SMRV was not significantly different from that of PCMRV (p = 0.951 for reviewer 1, and p = 0.999 for reviewer 2). CEMRV = single-phase contrast-enhanced MR venography, MRV = MR venography, PCMRV = phase-contrast MR venography, SMRV = subtraction MR venography

Table 2. Summation of Scores of Individual Venous Segments

	PCMRV	CEMRV	SMRV	*P*
Reviewer 1				
Dural sinuses (14 segments)	31, 25–34	50, 47–52*	48, 43–50*	< 0.001
Cerebral veins (5 segments)	9, 7–11	20, 16–20	16, 12–18	< 0.001
All segments (19 segments)	39, 34–45	68, 63–70	62, 60–67	< 0.001
Reviewer 2				
Dural sinuses (14 segments)	30, 23–32	49, 45–51*	47, 43–49*	< 0.001
Cerebral veins (5 segments)	10, 7–11	18, 17–20	15, 12–16	< 0.001
All segments (19 segments)	37, 32–42	66, 61–70	63, 57–64	< 0.001

Scores were presented with median and interquartile range. *P* values were acquired using Friedman test. Presented scores were sum of scores of 14 dural sinuses, 5 cerebral veins, and 19 all venous segments. Scoring system for each venous segment is follows: 4 for intense and continuous, 3 for faint and continuous, 2 for non-continuous with small gap, 1 for non-continuous with large gap, and 0 for non-visible. *Dural sinus score of CEMRV and SMRV were not significantly different in post hoc analysis ($p = 0.146$ in reviewer 1, and $p = 0.123$ in reviewer 2). CEMRV = single-phase contrast-enhanced MR venography, PCMRV = phase-contrast MR venography, SMRV = subtraction MR venography

in cerebral vein score. In contrast, the dural sinus scores of SMRV (median and IQR 48, 43–50 in reviewer 1, 47, 43–49 in reviewer 2) and CEMRV (median and IQR 50, 47–52 in reviewer 1, 49, 45–51 in reviewer 2) were not significantly different in the post hoc test ($p = 0.146$ in reviewer 1 and $p = 0.121$ in reviewer 2). Dural sinus scores of CEMRV and PCMRV (median and IQR 31, 25–34 in reviewer 1, 30, 23–32 in reviewer 2) were significantly different (Fig. 2).

There were significant differences in the SNR and CNR values among the three MRV techniques (Table 3). Post hoc testing suggested that the SNR and CNR of SMRV (median and IQR 104.5, 83.1–121.2 and 104.1, 74.9–120.5, respectively) were significantly higher than those of PCMRV (median and IQR 59.4, 49.2–74.9 and 53.6, 43.8–69.2, respectively) but lower than those of CEMRV (median and IQR 105.3, 111–182.6 and 148.4, 108–178.2, respectively) ($p = 0.043$). This result correlated well with image quality scores.

Representative cases are presented in Figures 3-5. A patient (Fig. 3) with a falx meningioma showed obliteration of the superior sagittal sinus on all three MRV images. Surgical findings confirmed the invasion of the meningioma into the superior sagittal sinus. Another patient (Fig. 4), who was undergoing follow-up after diagnosis of dural sinus thrombosis in the right transverse sinus, had a suspected persistent thrombosis on PCMRV. However, that segment was normal on both CEMRV and SMRV. There was also a case of a meningioma that had a feeding artery that mimicked a draining vein on conventional MRV (Fig. 5), but this structure was not seen on SMRV. After the review of dynamic TRMRA images, this vascular structure was confirmed to be a feeding artery to the meningioma and not a draining vein.

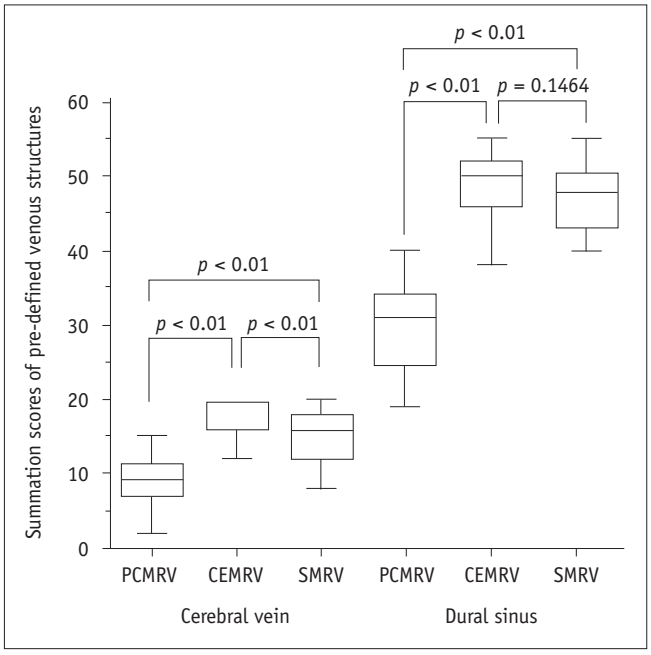

Fig. 2. Box plot of reviewer 1's cerebral vein and dural sinus scores of three MRVs. Presented *p* values were obtained from post hoc test (Wilcoxon signed rank test with Bonferroni correction). CEMRV = single-phase contrast-enhanced MR venography, MRV = MR venography, PCMRV = phase-contrast MR venography, SMRV = subtraction MR venography

DISCUSSION

Our results suggested the feasibility of SMRV for visualizing venous structures in the head and neck area. SMRV was acquired from post-processing TRMRA, which had the clinical utility to evaluate the intracranial venous system (4, 6, 7, 17). SMRV showed vein-only images in almost all cases, which was not achieved in the other MRV

Korean Journal of Radiology
KJR

techniques. The image quality of SMRV was comparable with that of other standard MRV methods used for visualizing intracranial venous structures. Assessment of major venous structures was possible with SMRV and was similar to current standard MRV methods.

One of the main benefits of SMRV is acquisition time. It is a post-processing result of TRMRA, and there is no need for additional imaging. Compared with other standard MRVs, TRMRA has a considerably short acquisition time (1 minute in our cases). In addition, TRMRA and SMRV were relatively insensitive to timing after bolus injection of contrast media. If the acquired CEMRV image is suboptimal because of timing or bolus problems (Fig. 4), it is difficult to re-acquire a CEMRV immediately. In contrast, SMRV with acceptable image quality could be obtained from post-processing TRMRA by selecting optimal A and B phases. Moreover, as with the protocol used in this study, SMRV could be successfully acquired from TRMRA with low-dose contrast media.

Previous reports discussed the clinical potential of TRMRA for assessing intracranial venous structures (5-7, 17). However, those studies did not address arterial contamination, which could hamper visualization of the venous structures. Arterial contamination cannot be avoided on venous phase images of currently available TRMRA methods. A major factor that contributes to this limitation is a longer temporal footprint to update time (12). Removing the arterial signal is beneficial for detailed assessment not only of venous structures, which are usually parallel to arteries, but also of unexpected arterial structures that mimic veins (Fig. 5). From this perspective, the SMRV has potential clinical benefit; it removed arterial structures successfully in nearly all cases (20/21), and the results were better than current standard MRV methods and TRMRA itself. Current MRV methods employ different strategies to suppress arterial signal; CEMRV uses imaging timing, and PCMRV uses optimal VENC settings and application of a saturation band (13, 18). Despite these methods, our results suggested that CEMRV and PCMRV still have suboptimal removal of arterial signal. Although a certain degree of arterial contamination was accepted in the clinical setting, better removal of arterial structures was needed for venous system evaluation.

Subtraction of two sets of images helped in visualizing

Table 3. SNR and CNR of MR Venographies

	PCMRV	CEMRV	SMRV	*P*
SNR	59.4, 49.2–74.9*	150.3, 111.0–182.6†	104.5, 83.1–121.2‡	< 0.001
CNR	53.6, 43.8–69.2*	148.4, 108.0–178.2†	104.1, 74.9–120.5‡	< 0.001

SNR and CNR were median and interquartile range. *P* values were acquired using Friedman test. Post-hoc analysis shows significant differences of SNR and CNR between different MRVs. *†‡Numbers with same superscripts in each row represent those are not significantly different in post hoc analysis. CEMRV = single-phase contrast-enhanced MR venography, CNR = contrast-to-noise ratio, MRV = MR venography, PCMRV = phase-contrast MR venography, SMRV = subtraction MR venography, SNR = signal-to-noise ratio

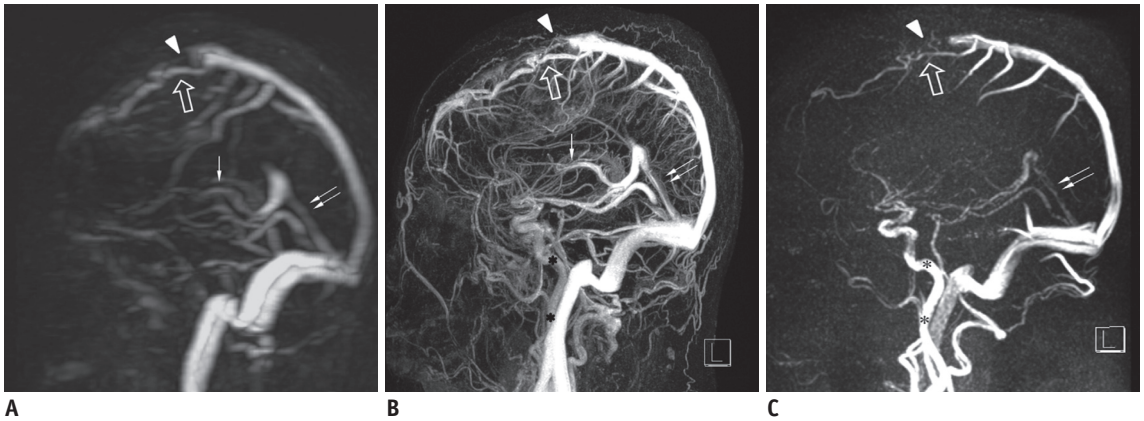

Fig. 3. 47-year-old female underwent MRV as part of her preoperative workup for midline meningioma.
PCMRV **(A)**, CEMRV **(B)**, and SMRV **(C)** reveal abrupt obliteration of superior sagittal sinus (arrowheads) and prominent collateral cortical vein (empty arrows). Note unsuppressed signal of internal carotid arteries in PCMRV and CEMRV (asterisks), whereas internal carotid arteries are not seen on SMRV. Internal cerebral veins (arrows) are not visualized on PCMRV. Degree of visualization of straight sinus (double arrows) and vein of Galen are different in three MRV images. CEMRV = single-phase contrast-enhanced MR venography, MRV = MR venography, PCMRV = phase-contrast MR venography, SMRV = subtraction MR venography

subtle enhancement or interval changes (19-22). This benefit of subtraction was commonly used for image processing in radiology. One of the major applications was angiographic images, including digital subtraction angiography (23). The basic concept underlying SMRV stemmed from this idea. Although SMRV had lower spatial resolution than other MRV methods, the image quality and ease of vein visualization were similar to or better than currently standard MRV techniques. Moreover, subtle structures were visualized more clearly, such as

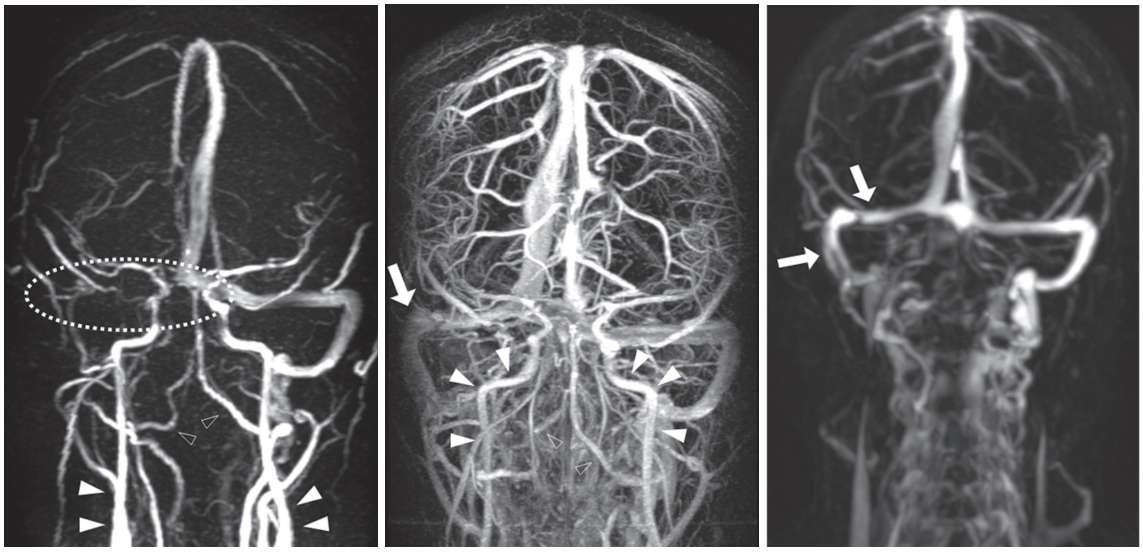

Fig. 4. 33-year-old man underwent follow-up MRV after diagnosis and treatment of right transverse sinus thrombosis.
Right transverse sinus, sigmoid sinus, jugular bulb and even proximal internal jugular vein are not visualized (dotted circle) on PCMRV **(A)**, and persistent thrombosis or stenosis could be suspected. Note arterial contamination (solid and empty arrowheads) on PCMRV. For this patient, timing of CEMRV **(B)** was suboptimal, and profound contamination of arterial structures (solid and empty arrowheads) and relatively weaker venous structure signal were observed. However, SMRV **(C)** enables clear visualization without contamination of arterial structures. Note clear visualization of right transverse and sigmoid sinuses (arrows). In addition, SMRV reveals very prominent paraspinal venous plexus. CEMRV = single-phase contrast-enhanced MR venography, MRV = MR venography, PCMRV = phase-contrast MR venography, SMRV = subtraction MR venography

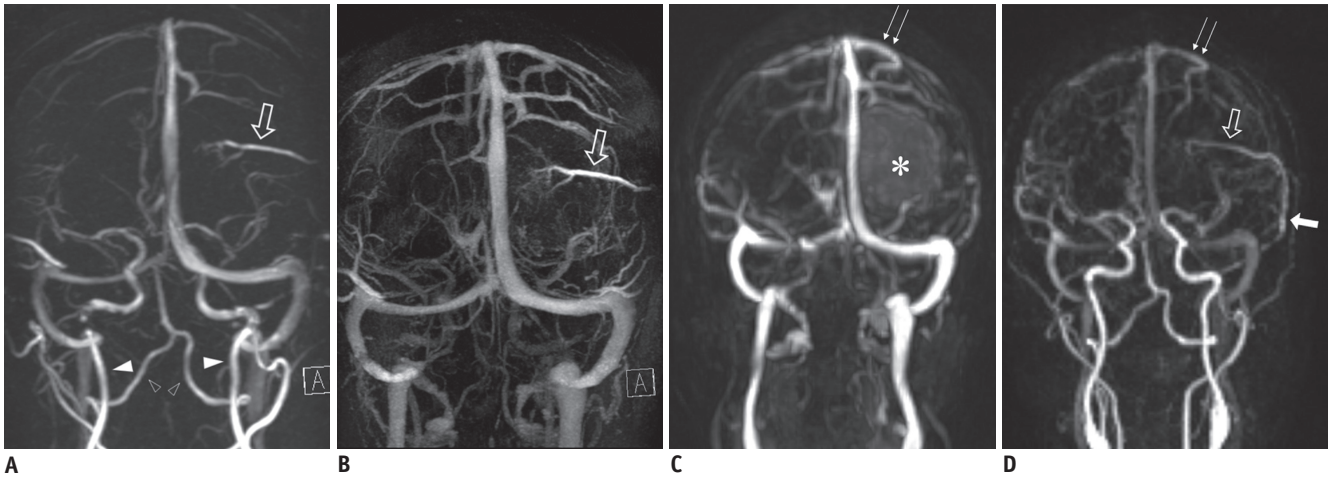

Fig. 5. 59-year-old female underwent MRV for preoperative workup of left parasagittal meningioma.
On PCMRV **(A)**, there is transverse vascular signal (empty arrow) where meningioma is located. Same vascular structure (empty arrow) is seen on CEMRV **(B)**. Vascular structure visualized on two conventional MRV was thought to be draining vein from meningioma. On SMRV **(C)**, this vascular structure is not seen. Instead, enhancing meningioma (asterisk) and tortuous cortical vein (double arrows) in superior aspect of meningioma are noted. TRMRA of arterial phase **(D)** reveals feeding artery (empty arrow) from middle meningeal artery (solid arrow), which is suspected as draining vein on conventional MRV. Note arterial contamination (solid and empty arrowheads) on PCMRV. CEMRV = single-phase contrast-enhanced MR venography, MRV = MR venography, PCMRV = phase-contrast MR venography, SMRV = subtraction MR venography, TRMRA = time-resolved contrast-enhanced MR angiography

Korean Journal of Radiology
KJR

the cavernous sinus and inferior petrosal sinus and the internal cerebral vein and straight sinus, which are not usually visualized on PCMRV. In addition, SMRV improved visualization of narrowed venous structures with slow flow. From this point of view, SMRV had sufficient contrast between venous structures and background, although it has inferior spatial resolution to that of current standard MRVs.

The subtraction process should remove only unwanted arterial signals, and targeted structures should remain untouched. For this purpose, choosing the two most appropriate phases is crucial. Generally, there was substantial visualization of venous structures on the arterial peak phase image. To avoid loss of venous structure signal throughout the subtraction process, we chose a phase with minimal venous signal (phase A) rather than arterial peak signal. Although the signal of the arterial structures was not at its peak, it was still substantial and sufficient to enable removing the arterial signal in phase B. As a result, the dural sinus score and cortical vein score of SMRV were better than those of PCMRV, and the dural sinus score of SMRV was comparable with that of CEMRV. Arterial signal was noted in only one case with arterial contamination on SMRV caused by subtle visualization of both vertebral arteries. The internal carotid arteries were not visualized, likely owing to the difference in flow velocity between the vertebral and internal carotid arteries (24, 25). However, the common and internal carotid arteries were out of the field of view of the standard MRV methods.

Time-resolved contrast-enhanced MR angiography could provide anatomical and hemodynamic information simultaneously (4, 10-12). However, it is not easy to achieve high temporal and spatial resolution simultaneously. In our institution, because hemodynamic information could be only obtained by TRMRA, TRMRA was acquired with high temporal resolution at the expense of spatial resolution. As a result, TRMRA in this study has lower spatial resolution than CEMRV. Different spatial resolution could be a reason for the inferior image quality and venous structure visualization of SMRV compared with CEMRV, which had better spatial resolution than TRMRA and SMRV. Future MRA with higher acceleration with higher parallel factors or compressed sensing might improve spatial resolution of TRMRA (26, 27).

Interestingly, SMRV enabled visualizing the venous drainage route of the head and neck in addition to intracranial venous structures. Because our TRMRA had supra-aortic fields of view, and the acquired SMRV images visualized supra-aortic venous structures. Imaging the venous structure of the neck area is challenging because of inter-individual variation and intra-individual physiologic changes (28-31). A few reports suggested the value of TRMRA for evaluating head and neck venous structures, especially in patients with multiple sclerosis (5, 8, 9). However, without sufficient arterial suppression, it is difficult to differentiate between neck veins and arteries. For this purpose, SMRV could be helpful as an imaging tool for veins in the neck area as well as for intracranial veins.

There are a number of limitations to our study. First, the study's retrospective design might have introduced unpredictable biases. Included patients were heterogeneous in terms of clinical indications for MRV and its findings. However, this suggested the clinical utility of SMRV with various clinical indications. In addition, we could not compare the SMRV with TOF MRV, another commonly used MRV method. Because of limited MR examination time, TOF MRV was not included in the routine MRV protocol in our hospital. Future study to compare SMRV with TOF MRV is needed. No patient underwent confirmative catheter venography. That invasive procedure is not routinely performed in our institution, and no patient was referred for catheter venography by clinicians. We did not compare SMRV and the venous phase of TRMRA. However, as mentioned earlier, SMRV is a post-processing result of TRMRA data, not a competitor. Although SMRV was suggested as a stand-alone MRV in our study, if applied in clinical practice, it could also serve as an additional and complementary image set to TRMRA images for venous system assessment; this is why we compared the SMRV with other standard MRV methods and not TRMRA. Although we presented a new SMRV for visualizing intracranial and neck area venous structures, further study regarding the diagnostic accuracy of SMRV for diseases involving intracranial and neck veins is needed.

In conclusion, SMRV is a practical method for visualizing venous structures obtained from TRMRA, without additional acquisition of specialized venography sequence. The image quality of SMRV is acceptable for clinical utility and comparable with that of other clinically used MRV methods. SMRV removed arterial contamination successfully in almost all cases.

REFERENCES

1. Ayanzen RH, Bird CR, Keller PJ, McCully FJ, Theobald MR,

Heiserman JE. Cerebral MR venography: normal anatomy and potential diagnostic pitfalls. *AJNR Am J Neuroradiol* 2000;21:74-78
2. Liauw L, van Buchem MA, Spilt A, de Bruïne FT, van den Berg R, Hermans J, et al. MR angiography of the intracranial venous system. *Radiology* 2000;214:678-682
3. Dolic K, Siddiqui AH, Karmon Y, Marr K, Zivadinov R. The role of noninvasive and invasive diagnostic imaging techniques for detection of extra-cranial venous system anomalies and developmental variants. *BMC Med* 2013;11:155
4. Meckel S, Reisinger C, Bremerich J, Damm D, Wolbers M, Engelter S, et al. Cerebral venous thrombosis: diagnostic accuracy of combined, dynamic and static, contrast-enhanced 4D MR venography. *AJNR Am J Neuroradiol* 2010;31:527-535
5. Zivadinov R, Lopez-Soriano A, Weinstock-Guttman B, Schirda CV, Magnano CR, Dolic K, et al. Use of MR venography for characterization of the extracranial venous system in patients with multiple sclerosis and healthy control subjects. *Radiology* 2011;258:562-570
6. Meckel S, Glücker TM, Kretzschmar M, Scheffler K, Radü EW, Wetzel SG. Display of dural sinuses with time-resolved, contrast-enhanced three-dimensional MR venography. *Cerebrovasc Dis* 2008;25:217-224
7. Yiğit H, Turan A, Ergün E, Koşar P, Koşar U. Time-resolved MR angiography of the intracranial venous system: an alternative MR venography technique. *Eur Radiol* 2012;22:980-989
8. McTaggart RA, Fischbein NJ, Elkins CJ, Hsiao A, Cutalo MJ, Rosenberg J, et al. Extracranial venous drainage patterns in patients with multiple sclerosis and healthy controls. *AJNR Am J Neuroradiol* 2012;33:1615-1620
9. Rahman MT, Sethi SK, Utriainen DT, Hewett JJ, Haacke EM. A comparative study of magnetic resonance venography techniques for the evaluation of the internal jugular veins in multiple sclerosis patients. *Magn Reson Imaging* 2013;31:1668-1676
10. Lim RP, Shapiro M, Wang EY, Law M, Babb JS, Rueff LE, et al. 3D time-resolved MR angiography (MRA) of the carotid arteries with time-resolved imaging with stochastic trajectories: comparison with 3D contrast-enhanced Bolus-Chase MRA and 3D time-of-flight MRA. *AJNR Am J Neuroradiol* 2008;29:1847-1854
11. Lee YJ, Laub G, Jung SL, Yoo WJ, Kim YJ, Ahn KJ, et al. Low-dose 3D time-resolved magnetic resonance angiography (MRA) of the supraaortic arteries: correlation with high spatial resolution 3D contrast-enhanced MRA. *J Magn Reson Imaging* 2011;33:71-76
12. Haider CR, Hu HH, Campeau NG, Huston J 3rd, Riederer SJ. 3D high temporal and spatial resolution contrast-enhanced MR angiography of the whole brain. *Magn Reson Med* 2008;60:749-760
13. Nael K, Fenchel M, Salamon N, Duckwiler GR, Laub G, Finn JP, et al. Three-dimensional cerebral contrast-enhanced magnetic resonance venography at 3.0 Tesla: initial results using highly accelerated parallel acquisition. *Invest Radiol* 2006;41:763-768
14. Lee YJ, Kim BS, Koo JS, Kim BY, Jang J, Choi HS, et al. Supra-aortic low-dose contrast-enhanced time-resolved magnetic resonance (MR) angiography at 3 T: comparison with time-of-flight MR angiography and high-resolution contrast-enhanced MR angiography. *Acta Radiol* 2015;56:673-680
15. Ruhl KM, Katoh M, Langer S, Mommertz G, Guenther RW, Niendorf T, et al. Time-resolved 3D MR angiography of the foot at 3 T in patients with peripheral arterial disease. *AJR Am J Roentgenol* 2008;190:W360-W364
16. Niendorf T, Sodickson DK. Parallel imaging in cardiovascular MRI: methods and applications. *NMR Biomed* 2006;19:325-341
17. Zivadinov R, Galeotti R, Hojnacki D, Menegatti E, Dwyer MG, Schirda C, et al. Value of MR venography for detection of internal jugular vein anomalies in multiple sclerosis: a pilot longitudinal study. *AJNR Am J Neuroradiol* 2011;32:938-946
18. Fera F, Bono F, Messina D, Gallo O, Lanza PL, Auteri W, et al. Comparison of different MR venography techniques for detecting transverse sinus stenosis in idiopathic intracranial hypertension. *J Neurol* 2005;252:1021-1025
19. Boetes C, Barentsz JO, Mus RD, van der Sluis RF, van Erning LJ, Hendriks JH, et al. MR characterization of suspicious breast lesions with a gadolinium-enhanced TurboFLASH subtraction technique. *Radiology* 1994;193:777-781
20. Anxionnat R, Bracard S, Ducrocq X, Trousset Y, Launay L, Kerrien E, et al. Intracranial aneurysms: clinical value of 3D digital subtraction angiography in the therapeutic decision and endovascular treatment. *Radiology* 2001;218:799-808
21. Sugahara T, Korogi Y, Nakashima K, Hamatake S, Honda S, Takahashi M. Comparison of 2D and 3D digital subtraction angiography in evaluation of intracranial aneurysms. A*JNR Am J Neuroradiol* 2002;23:1545-1552
22. Uemura M, Miyagawa M, Yasuhara Y, Murakami T, Ikura H, Sakamoto K, et al. Clinical evaluation of pulmonary nodules with dual-exposure dual-energy subtraction chest radiography. *Radiat Med* 2005;23:391-397
23. Chilcote WA, Modic MT, Pavlicek WA, Little JR, Furlan AJ, Duchesneau PM, et al. Digital subtraction angiography of the carotid arteries: a comparative study in 100 patients. *Radiology* 1981;139:287-295
24. Acar M, Degirmenci B, Yucel A, Albayrak R, Haktanir A. An evaluation of internal carotid artery and cerebral blood flow volume using color duplex sonography in patients with vertebral artery hypoplasia. *Eur J Radiol* 2005;53:450-453
25. Ford MD, Alperin N, Lee SH, Holdsworth DW, Steinman DA. Characterization of volumetric flow rate waveforms in the normal internal carotid and vertebral arteries. *Physiol Meas* 2005;26:477-488
26. Jung H, Sung K, Nayak KS, Kim EY, Ye JC. k-t FOCUSS: a general compressed sensing framework for high resolution dynamic MRI. *Magn Reson Med* 2009;61:103-116
27. Rapacchi S, Natsuaki Y, Plotnik A, Gabriel S, Laub G, Finn JP, et al. Reducing view-sharing using compressed sensing in time-resolved contrast-enhanced magnetic resonance angiography. *Magn Reson Med* 2015;74:474-481

28. Andeweg J. The anatomy of collateral venous flow from the brain and its value in aetiological interpretation of intracranial pathology. *Neuroradiology* 1996;38:621-628
29. Kudo K, Terae S, Ishii A, Omatsu T, Asano T, Tha KK, et al. Physiologic change in flow velocity and direction of dural venous sinuses with respiration: MR venography and flow analysis. *AJNR Am J Neuroradiol* 2004;25:551-557
30. Schaller B. Physiology of cerebral venous blood flow: from experimental data in animals to normal function in humans. *Brain Res Brain Res Rev* 2004;46:243-260
31. Kopelman M, Glik A, Greenberg S, Shelef I. Intracranial nonjugular venous pathways: a possible compensatory drainage mechanism. *AJNR Am J Neuroradiol* 2013;34:1348-1352